TECHNICAL MEMORANDUM MAN-63-65

LIQUID METAL CONDENSATION

Jon Lee

December 1963

AIR FORCE MATERIALS LABORATORY
RESEARCH AND TECHNOLOGY DIVISION
AIR FORCE SYSTEMS COMMAND
WRIGHT-PATTERSON AIR FORCE BASE, OHIO

PROJECT 7340, TASK: 734008

REPORT DOCUMENTATION PAGE			Form Approved OMB No. 0704-0188

1. AGENCY USE ONLY *(Leave blank)*	2. REPORT DATE	3. REPORT TYPE AND DATES COVERED
	DECMBER 1963	FINAL JANUARY - OCTOBER 1963

4. TITLE AND SUBTITLE
LIQUID METAL CONDENSATION

5. FUNDING NUMBERS

6. AUTHOR(S)
JON LEE

7. PERFORMING ORGANIZATION NAME(S) AND ADDRESS(ES)
NONMETALLIC MATERIALS DIVISION
AIR FORCE MATERIALS LABORATORY
RESEARCH AND TECHNOLOGY DIVISION
AIR FORCE SYSTEMS COMMAND
WRIGHT-PATTERSON AFB, OH 45433

8. PERFORMING ORGANIZATION REPORT NUMBER

9. SPONSORING/MONITORING AGENCY NAME(S) AND ADDRESS(ES)
NONMETALLIC MATERIALS DIVISION
AIR FORCE MATERIALS LABORATORY
RESEARCH AND TECHNOLOGY DIVISION
AIR FORCE SYSTEMS COMMAND
WRIGHT-PATTERSON AFB, OH 45433

10. SPONSORING/MONITORING AGENCY REPORT NUMBER
TECHNICAL MEMORANDUM
MAN 63-65

11. SUPPLEMENTARY NOTES

12a. DISTRIBUTION AVAILABILITY STATEMENT
APPROVED FOR PUBLIC RELEASE; DISTRIBUTION UNLIMITED

12b. DISTRIBUTION CODE

13. ABSTRACT *(Maximum 200 words)*
A STUDY OF TURBULENT FILM CONDENSATION WAS FIRST MADE BASED ON THE TWO-PHASE MODEL UTILIZING THE EDDY KINEMATIC VISCOSITIES OF DEISSLER AND VON KARMAN. IT HAS BEEN SHOWN THAT THE PREDICTION OF THE AVERAGE HEAT TRANSFER COEFFICIENT IS STILL HIGHER THAN THE LIQUID METAL DATA OF MISRA AND BONILLA. UNDER THE PREMISE THAT AN UPWARD VAPOR FLOW CAN GREATLY REDUCE THE HEAT TRANSFER COEFFICIENT. THE OBSERVED SCATTER OF DATA MAY BE ATTRIBUTABLE TO THE VARIATIONS OF VAPRO VELOCITY.

14. SUBJECT TERMS
LUBRICATION, MECHANICAL WEAR

15. NUMBER OF PAGES
28

16. PRICE CODE

17. SECURITY CLASSIFICATION OF REPORT	18. SECURITY CLASSIFICATION OF THIS PAGE	19. SECURITY CLASSIFICATION OF ABSTRACT	20. LIMITATION OF ABSTRACT
UNCLASSIFIED	UNCLASSIFIED	UNCLASSIFIED	SAR

FOREWORD

This report was prepared by the Fluid and Lubricant Materials Branch, Nonmetallic Materials Division, AF Materials Laboratory, Research and Technology Division with Jon Lee as project engineer. The work reported herein was initiated under Project No. 7340, "Nonmetallic and Composite Materials", Task No. 734008, "Power Transmission Heat Transfer Fluids".

This report covers the partial work done during the period from January 1963 to October 1963.

ABSTRACT

A study of turbulent film condensation was first made based on the two-phase model utilizing the eddy kinematic viscosities of Deissler and von Karman. It has been shown that the prediction of the average heat transfer coefficient is still higher than the liquid metal data of Misra and Bonilla. Under the premise that an upward vapor flow exists, it has been shown qualitatively that an upward vapor flow can greatly reduce the heat transfer coefficient. The observed scatter of data may be attributable to the variations of vapor velocity.

This report has been reviewed and is approved.

R. L. ADAMCZAK, Chief
Fluid & Lubricant Materials Branch
Nonmetallic Materials Division
AF Materials Laboratory

Introduction

In a recent paper [4]* using Nusselt's model, the author has made an investigation of turbulent film condensation by utilizing the eddy kinematic viscosity expressions of Deissler and von Karman. A few important conclusions, which are relevant to liq... metals, were that (i) the heat transfer coefficients (with respect to Reynolds number) approach a limit as Prandtl number becomes small, (ii) the limit is not too much different from Nusselt's laminar case, and (iii) the results are rather insensitive to the value of the ratio of eddy thermal diffusivity to eddy kinematic viscosity. Conclusion (iii) is a collorary of (i) which implies that the magnitude of the molecular thermal conductivity is dominant over that of the eddy conductivity in the small Prandtl **number** range. Conclusion (ii) is not very encouraging from the practical standpoint because the experimental data are much lower than the prediction based upon Nusselt's laminar model. Therefore, it was mentioned in that paper [4] that a proper description of the problem must include the following modifications: (a) non-vanishing interfacial shear stress, (b) inertia effects, (c) convective heat transfer and subcooling, (d) interfacial waves and rippling, (e) interfacial thermal resistance, and (f) contact thermal resistance.

The purpose of this paper is to investigate the turbulent condensation by including the first three modifications. The problem can be formulated within the framework of a two-phase boundary layer treatment, and the interfacial shear stress is that caused by a quiescent vapor at infinity. This type of problem has already been worked out by others [1, 2, 3] but only for the laminar case. Therefore, the feature of the present analysis is to inc-

***) Numbers in brackets refer to the References at the end of the paper.**

lude the effect of turbulent transports in a two-phase film condensation model. A discussion will also be presented, which will offer an explanation for discrepancy between the theoretical predictions and the experimental data.

Formulation

The physical model for film-wise condensation is as shown in Figure 1, where the x-axis is parallel and the y-axis is perpendicular to the plate. Suppose a semi-infinite plate is immersed in a quiescent, saturated vapor. If the plate is held at a lower temperature t_w than that of the vapor t_s, the vapor will condense and a film of condensate will flow downward due to gravity. At the interface of the condensate and vapor, a motion will be induced in the vapor due to a shearing action of the condensate and thus a vapor boundary layer will be formed.

Under the assumption that the variation of physical properties can be ignored within the temperature range involved, we can write the following boundary layer equations:

Condensate:

(1) $$\frac{\partial u}{\partial x} + \frac{\partial v}{\partial y} = 0$$

(2) $$u\frac{\partial u}{\partial x} + v\frac{\partial u}{\partial y} = g + \frac{\partial}{\partial y}\left(\nu_t \frac{\partial u}{\partial y}\right)$$

(3) $$u\frac{\partial t}{\partial x} + v\frac{\partial t}{\partial y} = \frac{\partial}{\partial y}\left(\kappa_t \frac{\partial t}{\partial y}\right)$$

Vapor:

$$\frac{\partial \hat{u}}{\partial x} + \frac{\partial \hat{v}}{\partial y} = 0 \tag{4}$$

$$\hat{u}\frac{\partial \hat{u}}{\partial x} + \hat{v}\frac{\partial \hat{u}}{\partial y} = \frac{\partial}{\partial y}\left(\hat{\nu}_t \frac{\partial \hat{u}}{\partial y}\right) \tag{5}$$

where ν_t and K_t denote the total kinematic viscosity and total thermal diffusivity. We shall impose the following conditions:

$u = v = 0$ and $t = t_w$ at $y = 0$

$t = t_s$ at $y = \delta$

$\hat{u} = \hat{v} = 0$ and $t = t_s$ at $y = \infty$

Since a constant temperature will be assumed in the vapor, the equation of heat energy does not appear in that layer.

At the interface, we also demand the continuity of velocity, shear stress, and mass flux, as:

$$u(\delta) = \hat{u}(\delta)$$

$$\mu_t\,(\partial u/\partial y)_\delta = \hat{\mu}_t\,(\partial \hat{u}/\partial y)_\delta$$

$$\rho\,\frac{\partial}{\partial x}\int_0^\delta u\,dy = -\hat{\rho}\,\frac{\partial}{\partial x}\int_\delta^\infty \hat{u}\,dy$$

As a useful approximation, it has been shown [1, 3] that the fulfillment of the above interfacial conditions can be achieved satisfactorily by simply considering the following relationship:

$$u(\delta)\frac{\partial}{\partial x}\int_0^\delta u\,dy + \nu_t\left(\frac{\partial u}{\partial y}\right)_\delta = 0 \tag{6}$$

Therefore, without solving $\hat{u}$ explicitly, this allows us to investigate the two-phase condensation by treating only the equations in the condensate layer.

Method of Solution

The condensation problem can be characterized by introducing an integral relation which states that the increase in the condensate flow rate is entirely due to the vapor being condensed:

$$(7) \qquad \frac{\lambda}{c_p}\frac{\partial}{\partial x}\int_0^\delta u\,dy - K_t\left(\frac{\partial t}{\partial y}\right)_\delta = 0$$

Since conditions (6) and (7) are already in an integral form, it is convenient to convert (2) and (3) into a similar form. If equations (2) and (3) are integrated in y from $\delta \longrightarrow y$ and conditions (6) and (7) are incorporated, we obtain:

$$(8) \quad 2\int_y^\delta u(\partial u/\partial x)dy + u\int_0^y(\partial u/\partial x)dy + u^2(\delta)(d\delta/dx) - g(\delta - y) + \vartheta_t(\partial u/\partial y) = 0$$

$$(9) \quad \int_y^\delta u(\partial\theta/\partial x)dy - \int_y^\delta(1-\theta)(\partial u/\partial x)dy - (1-\theta)\int_0^y(\partial u/\partial x)dy - $$
$$-(\lambda/c_p\,\Delta t)\left\{\int_0^\delta(\partial u/\partial x)dy + u(\delta)(d\delta/dx)\right\} + K_t(\partial\theta/\partial y) = 0$$

where $\theta = t - t_w/\Delta t$. The use of continuity equation (1) has been made in eliminating v's in the above.

Following the spirit of a phenomenological approach, the total transport coefficients are assumed to be the sum of two contributions - molecular and eddy. As in the previous work [4], we shall adopt the eddy kinematic viscosities of Deissler and von Karman and let the ratio of eddy thermal diffusivity to eddy kinematic viscosity be a constant. The assumption of a constant ratio may be criticized because of its dependency on the Peclet number and the flow geometry. However, this serves for our present purpose of attempting to assess a gross effect of turbulent transports - more will be said later.

Near the plate, we have Deissler's expression for eddy kinematic viscosity as:

$$(10) \qquad \nu_1^* = n^2\, u\, y\, (1 - \exp(-n^2 uy/\nu)) \qquad , 0 \leq y \leq y^*$$

and we have von Karman's expression, which is valid at a distance from the plate, as:

$$(11) \qquad \nu_2^* = K^2 \left| (du/dy)^3/(d^2u/dy^2)^2 \right| \qquad , y^* \leq y$$

where n, K, and y* are empirical constants.

In the laminar case, ν_t and κ_t are constants; therefore, a similarity transformation reduces equations (8) and (9) into a one-dimensional problem. However, in our case, such a simplification does not exist and, in general, ν_t and κ_t will introduce further non-linearity into the system. This suggests the necessity of treating the numerical solution as an initial-value problem. In doing so, it is advantageous to make a transformation such that the domain of u and Θ becomes rectangular instead of a wedge-shaped boundary layer. This can be done by introducing new coordinates, $\eta = y/\delta$ and $\xi = x$, then equations (8) and (9) become:

$$(12) \qquad 2\int_\eta^1 U(\partial U/\partial\xi)d\eta + U\int_0^\eta(\partial U/\partial\xi)d\eta + (\delta'/\delta)\left\{\int_\eta^1 U^2\, d\eta + U\int_0^\eta U d\eta\right\} -$$

$$- g(1 - \eta) + (\nu_t/\delta^2)(\partial U/\partial\eta) = 0$$

$$(13)\qquad \int_\eta^1 U(\partial T/\partial\xi)d\eta + \int_\eta^1 \tau(\partial U/\partial\xi)d\eta + \tau\int_0^\eta(\partial U/\partial\xi)d\eta + (\delta'/\delta)\left\{\tau\int_0^\eta U\,d\eta + \int_\eta^1 \tau U\,d\eta\right\} + (K_t/\delta^2)(\partial T/\partial\eta) = 0$$

where $\tau = (T - 1) - \dfrac{\lambda}{C_p\,\Delta t}$ and $\delta' = d\delta/d\xi$.

Numerical Procedure

In a plane of ξ and η, the set of equations (12) and (13) can be converted into a system of partial differential equations. This is done by first setting up a two-dimensional mesh in $\Delta\xi$ and $\Delta\eta$ (see Figure 2). Since $0 \le \eta \le 1$, the total number of η-mesh, N, will be assigned ab initio. If the integrals in (12) and (13) are approximated by the trapezoidal rule, each equation gives rise to a system of N partial differential equations - 2N for the total. That is, equations (12) and (13) can be written as:

$$(14)\qquad 2\Delta\eta\sum_n^N \sigma U_i(\partial U/\partial\xi)_i + U_n\Delta\eta\sum_0^n \sigma(\partial U/\partial\xi)_i + (d\delta/d\xi)(\Delta\eta/\delta)\left\{\sum_n^N \sigma U_i^2 + U_n\sum_0^n \sigma U_i\right\} - g(1 - n\cdot\Delta\eta) + ((\vartheta_t)_n/\delta^2)(\partial U/\partial\eta)_n = 0$$

$$(15)\qquad \Delta\eta\sum_n^N \sigma U_i(\partial T/\partial\xi)_i + \Delta\eta\sum_n^N \sigma\tau_i(\partial U/\partial\xi)_i + \tau_n\Delta\eta\sum_0^n \sigma(\partial U/\partial\xi)_i + (d\delta/d\xi)(\Delta\eta/\delta)\left\{\tau_n\sum_0^n \sigma U_i + \sum_n^N \sigma\tau_i U_i\right\} + ((K_t)_n/\delta^2)(\partial T/\partial\eta)_n = 0$$

where σ is 1/2 for the first and last terms of a sum and 1 for all others. For (14) there are N+1 unknowns, $(\partial U/\partial\xi)_1, \cdots, (\partial U/\partial\xi)_N$ and $(d\delta/d\xi)$, because $(\partial U/\partial\xi)_o$ vanishes. On the other hand, since $(\partial T/\partial\xi)_o$ and $(\partial T/\partial\xi)_N$ vanish, there are only N-1 unknowns, $(\partial T/\partial\xi)_1, \cdots, (\partial T/\partial\xi)_{N-1}$, for (15). Therefore, we have a consistent system of 2N partial differential equations, each of which is of the following form:

$$\text{(16)} \qquad \frac{\partial f}{\partial \xi} = F(U,T,\delta,\nu_t,\kappa_t)\frac{\partial f}{\partial \eta}$$

where f denotes U, T, or δ.

With conditions at $\xi = \xi_o$, this is an initial-value problem of tracing the ξ-evolution of f. Since equation (16) was originated from the parabolic boundary layer equations, it can be considered as a psuedo-diffusion type equation with a variable, non-linear diffusion coefficient. An implicit scheme will then be used in writing (16) in a finite difference form, as:

$$\text{(17)} \qquad f_n^{k+1} - f_n^{k} \;/\Delta\xi = F_n^{k}\,(\, f_{n+1}^{k+1} - f_{n-1}^{k+1} \;/\Delta\eta\,)$$

From the standpoint of convergence and stability, the implicit scheme is considered to be superior to the explicit one, but this is always achieved at the expense of extra labors. However, this is not true in our case because equations (14) and (15) must be treated as a system of equations, preferably linear. At any rate, no additional work has been incurred. In the interest of simplicity, equation (17) was linearized by taking F_n^k rather than an average, e.g. $(F_n^k + F_n^{k+1})/2$, which involves interations. The improvement in the final results did not justify the added complications.

The final finite difference equations based on an implicit scheme are:

$$(18)\quad U_n^k U_n^{k+1} + 2\sum_{n+1}^{N-1} U_i^k U_i^{k+1} + U_N^k U_N^{k+1} + (U_n^k/2)\Big\{2\sum_{1}^{n-1} U_i^{k+1} + U_n^{k+1}\Big\} +$$

$$+ \delta^{k+1}(1/2\,\delta^k)\Big\{(U_n^k)^2 + 2\sum_{n+1}^{N-1}(U_i^k)^2 + (U_N^k)^2 + U_n^k\Big(2\sum_{1}^{n-1}U_i^k + U_n^k\Big)\Big\} +$$

$$+(1/\delta^k)^2(\Delta\xi/2\,\Delta\eta^2)(\nu_t)_n^k\,(U_{n+1}^{k+1} - U_{n-1}^{k+1}) = g\,(1 - n\cdot\Delta\eta)(\Delta\xi/\Delta\eta) +$$

$$+(3/2)\Big\{(U_n^k)^2 + 2\sum_{n+1}^{N-1}(U_i^k)^2 + (U_N^k)^2\Big\} + U_n^k\Big(2\sum_{1}^{n-1}U_i^k + U_n^k\Big)$$

$$(19)\quad U_n^k T_n^{k+1} + 2\sum_{n+1}^{N-1} U_i^k T_i^{k+1} + U_N^k T_N^{k+1} + \tau_n^k U_n^{k+1} + 2\sum_{n+1}^{N-1}\tau_i^k U_i^{k+1} + \tau_N^k U_N^{k+1} +$$

$$+\tau_n^k\Big\{2\sum_{1}^{n-1}U_i^{k+1} + U_N^k\Big\} + (1/\delta^k)^2(\Delta\xi/\Delta\eta^2)(\kappa_t)_n^k\,(T_{n+1}^{k+1} - T_{n-1}^{k+1}) +$$

$$+\delta^{k+1}(1/\delta^k)\Big\{\tau_n^k\Big(2\sum_{1}^{n-1}U_i^k + U_n^k\Big) + \tau_n^k U_n^k + 2\sum_{n+1}^{N-1}\tau_i^k U_i^k + \tau_N^k U_N^k\Big\} =$$

$$= U_n^k T_n^k + 2\sum_{n+1}^{N-1}U_i^k T_i^k + U_N^k T_N^k + 2\tau_n^k\Big\{2\sum_{1}^{n-1}U_i^k + U_N^k\Big\} +$$

$$+2\Big\{\tau_n^k U_n^k + 2\sum_{n+1}^{N-1}\tau_i^k U_i^k + \tau_N^k U_N^k\Big\}$$

For our problem, any attempt to assess the a priori convergence by means of an amplification matrix [7] does not seem very practical. Therefore, we shall resort to a trial-and-error approach in that sufficiently small, yet not impractical, $\Delta\xi$ and $\Delta\eta$ will be chosen by testing the numerical results. This is also supported by Lax's theorem which states that the stability is the necessary and sufficient condition for convergence. The overall error bound for the present method can be estimated as $O(\Delta\xi) + O(\Delta\eta)$.

Equations (18) and (19) form a system of 2N linear equations in 2N unknowns, $U_1,\cdots,U_N$, $T_1,\cdots,T_{N-1}$, δ, at the forward step of ξ; and the augmented matrix can be determined from the information available at the backward step.

Numerical Results

The system of (18) and (19) was first studied for the laminar case by setting $\nu_t = \nu$ and $\kappa_t = \kappa$. The forward marching numerical solution was commenced at ξ_o(= 0.1 cm) with appropriately chosen initial conditions.* It is not the purpose of this paper to re-compute the laminar case; however, it provides an excellent check on the correctness and accuracy of the present numerical method. This was done by exploring the similarity of boundary layer equations; that is, a particular ξ-dependency exists so that certain quantities can be made invariant in ξ. For instance, $U/(g/\nu)$, T, and δ/δ_o (where $\delta_o = [4(C_p \Delta t/\lambda) \times /P_r (g/\nu^2)]^{1/4}$ is Nusselt's laminar film thickness) must be independent of ξ. Indeed, for the worst case, the constancy of the first 4-digits for $U/(g/\nu)$, 5- for T, and 3- for δ/δ_o, were observed. In addition, the laminar results will serve as the initial conditions for the turbulent case.

In this work, we shall restrict ourselves to computations for two Prandtl numbers, 0.008 and 0.003, which are typical of liquid metals. From the numerical standpoint, the use of (10) and (11) presents some difficulties. First, von Karman's expression requires the first and second derivatives of U and the numerical differentiation always amplifies the roughness of data. As $\partial U/\partial \eta$ must vanish once due to the upward (negative) interfacial drag, its magnitude also varies in a wide range. Another distracting feature was that

* First the numerical solution was started with the initial conditions corresponding to Nusselt's result. By similarity as the solution progresses in ξ, $U/(g/\nu^2)$, T, and δ/δ_o approach limiting values which are quite different from the initial conditions. The limiting values will then be used as the initial conditions for the final computations.

the stability seemed to be sensitive to the irregularities resulting from numerical differentiations. By trials, it was found that the consistent and conservative derivatives can be obtained by smoothing the data with a second degree least-square fit. Second, the values of eddy kinematic viscosities of (10) and (11) are not usually identical at y^*; therefore, there is a jump at that point. This is inherent in the present numerical method because such a difficulty can be mended rigorously in Nusselt's turbulent case [4]. Therefore, we have introduced the following artifice of smoothly connecting (10) and (11):

$$(20) \quad \nu^* = \nu_1^* \exp(-0.695(y/y^*)^5) + \nu_2^* (1 - \exp(-0.695(y/y^*)^5)$$

The above relationship does not have a theoretical justification and it will be considered as an expediency. At any rate, (20) reduces to $\nu^* \cong \nu_1^*$, for $y < y^*$ and $\nu^* \cong \nu_2^*$ for $y > y^*$, and to $\nu^* = (\nu_1^* + \nu_2^*)/2$ at y^*. The arbitrary exponent 5 tends to narrow the diffused range drastically. The introduction of the above remedies, however, does not conflict with our objectives, because the correct order of magnitude of eddy transport coefficients are maintained.

In all computations, the following values of parameters are used; $n = 0.124$, $K = 0.4$, $y^* = 23\nu/\sqrt{\tau_w/\rho}$, $\alpha = 1$, $\nu = 0.005\ \mathrm{cm}^2/\mathrm{sec}$, and $L = 20$ cm*. Some results of numerical computation will be shown here for $P_r = 0.008$ and $C_p\Delta t/\lambda = 0.01$. In Figure 3, the turbulent velocity profiles at $x = 10$ and 20 cm are compared with the laminar distribution. The effect of eddy kinematic viscosity is to flatten the velocity profile in general.

*) The particular choice of values for ν and L is immaterial to our results. In particular, the appearance of ν could have been eliminated completely by a proper transformation.

The laminar temperature profile is essentially linear and the turbulent ones seem to swing around the linear profile with small deviations as shown in Figure 4. In Figure 5, the film thicknesses for (a) Nusselt's laminar case, (b) the two-phase laminar case, and (c) the two-phase turbulent case are compared. Because of the existence of similarity, (a) and (b) are not only straight but displaced by a constant factor; while (c) deviates from (b) and increases rapidly with x.

Heat Transfer Results

The heat transfer coefficient for condendation is defined as:

(21) $$h = k(\partial t/\partial y)_w / \Delta t$$

which is obtained from the heat energy balance, $h\Delta t = k(\partial t/\partial y)_w$. In the absence of similarity, the dependency of the heat transfer coefficient on the plate length will be avoided by adopting the following parameters: Reynolds number:

(22) $$Re_L = 4\Gamma/\mu = (4/\nu)\int_0^{\delta} u\, dy \qquad \text{at } x = L$$

and, average heat transfer coefficient:

(23) $$(\nu^2/g)^{1/3} h_{av}/k = (\nu^2/g)^{1/3}(1/\Delta t\, L)\int_0^L (\partial t/\partial y)_w\, dx$$

For Nusselt's laminar case, the following relationship between Re_L and h_{av} exists:

(24) $$(\nu^2/g)\, h_{av}/k = 1.47\, Re_L^{-1/3}$$

In Figure 6, equation (24) was plotted as curve (1) and the results of Nusselt's turbulent case--taken from ref. [4]--were shown by curves (2) and (3), P_r = 0.01 and 0.001. The results of the present analysis are summarized in curves (4), (5), (6), and (7). Curves (4) and (5) are the results of the two-phase laminar case for P_r = 0.008 and 0.003 respectively. The results of the two-phase turbulent case are shown by curves (6) and (7) for the same Prandtl numbers. As in the previous work [4], the heat transfer results are not sensitive to the particular value of α and the average heat transfer coefficient is decreased by not more than 4% by taking $\alpha = 0.1$ as an example.

Discussions

Within the range of Re_L up to 2,000, which covers most of the experimental data of Misra and Bonilla [5], curves (2) and (3) show somewhat lower h_{av} than curve (1), but the difference is rather modest (about 10%). Similarly, the comparison of two pairs of curves, (4) with (6) and (5) with (7), indicates that the turbulent model reduced h_{av} roughly by the same fraction, i.e. 10%. From these comparisons one can conclude that the turbulent transports can reduce the heat transfer coefficient but only by a small fraction. This can be visualized from the fact that the increase of film thickness is counteracted by a smaller turbulent velocity so as to give approximately the same flow rate as in the laminar case. Therefore, any decrease in the heat transfer coefficient appears to be directly proportional to the increase in the film thickness, because $h \cong k/\delta$. However, the average effect (over L) is much weaker.

Nevertheless, one of the observations worthy of attention is that curves (4) and (5) can predict considerably lower h_{av} compared to curve (1). This is certainly attributable to the improvements over the Nusselt's model. One of the modifications notably the "non-vanishing interfacial shear stress", is believed to be mainly responsible for such reduction (see ref. [9]). All in all, the bulk of irregularly scattered data still lies well below all the curves, therefore, it seems logical to then ask what would be the effect of an upward vapor velocity in liquid metals condensation. This was motivated by the fact that the upward interfacial drag we have considered was caused by a quiescent vapor and the existance of upward vapor flow was observed by Misra and Bonilla. They have reported that, in some of the low-pressure film condensation runs, the vapor flow was large enough to blow off the film from the condenser plate in all directions. Nusselt [6] first studied the effect of upward vapor flows but his results are not suited for our discussion. Therefore, we shall present here a qualitative analysis on the effect of an upward vapor flow based on Nusselt's model. The equation of motion can be modified as:

(25) $$du/dy = g\,\delta\,(1 - y/\delta)/\nu - \tau_i/\nu\rho$$

where τ_i denotes the interfacial shear stress. In the interest of maintaining similarity, let us set $\tau_i/\rho = \beta g\,\delta$, then we have:

(26) $$du/dy = g\,\delta\,(1 - \beta)(1 - y/\delta(1-\beta))/\nu$$

where $0 < \beta < 2/3$ is assumed ($\beta < 2/3$ assures $\Gamma > 0$). In this way, the effect of upward velocity is related directly to the position of zero velocity gradient and for the case of quiescent vapor of Figure 3, $\beta \cong 0.3$ (for the laminar case). A detailed investigation of condensation using

(26) is rather involved because the character of solution changes as the interfacial shear stress increases. However, within the range of small upward vapor velocity, let us assume that the boundary condition of $\delta = 0$ at $x = 0$ is still valid. With a linear temperature profile and constant Δt, the relationship between Re_L and h_{av}, similar to (24) becomes:

$$(27) \qquad (\nu^2/g)^{1/3} h_{av}/k = 1.47 (1 - 3\beta/2)^{1/3} Re_L^{-1/3}$$

The above equation implies that h_{av} can be smaller by a factor of $(1-3\beta/2)^{1/3}$ in comparison to the Nusselt's laminar case (24). In Figure 6, equation (27) was plotted for several values of β. Curves (8), (9), (10), and (11) cover most of the data. It is seen that the upward vapor flow can cause the reduction of h_{av} and, consequently, the scatter of data could have been caused by the variations in vapor velocity. **This is in confirmity with the** previous findings of Colburn and Carpenter [10]. As one expects, h_{av} should increase with the positive (downward) interfacial shear stress [8]. However, it is very strange to note that the data of Misra and Bonilla are not consistent with the trend predicted by equation (27). In fact, they have observed that the data seem to approach equation (24) as the upward vapor velocity increases, but the data fall well below (24) when the upward vapor flow is small. They pointed out that these facts are "striking", but did not offer an explanation. It must be noted that the experimental data are not very accurate due to the unsurmountable experimental difficulties. In a few instances, the author was able to observe much higher h than the reported data value by making re-computations.

Conclusions

In an attempt to explain the discrepancy existing between the theoretical predictions and the experimental data for liquid metal condensation, the two-phase turbulent condensation was studied. As in the Nusselt's turbulent case, the inclusion of turbulent transports reduces the heat transfer coefficient. The overall effect is rather modest and the reduction of h_{av} does not exceed 10% over the laminar model within the experimental range of Re_L. In experiments, however, the presence of an upward vapor flow was observed, which was perhaps inevitable from the usual experimental set-up. It has been shown qualitatively that the upward vapor flow can reduce the heat transfer coefficients. Consequently, the scatter of data could have been caused by the variations in vapor velocity. In order to confirm the assertion proposed above, it is necessary to carry out an exact formulation of the problem so as to relate β to the vapor velocity directly and it is also necessary to measure the accurate local vapor velocity in condensation.

Nomenclatures

C_p	Specific heat at constant pressure
g	$g'\Delta\rho/\rho$
g'	acceleration due to gravity
h	heat transfer coefficient for condensation
K	von Karman's constant
k	thermal conductivity
L	plate length
n	Deissler's constant
P_r	Prandtl number
R_e	Reynolds number
t	temperature
Δt	$t_s - t_w$
T	temperature in ξ and η
u, v	velocity components in x and y
U	velocity component u in ξ and η
x, y	coordinate system (physical)
y^*	separation of Deissler and von Karman regions

Greeks

α	κ^* / ν^*
β	see equation 26
γ	shear stress
Γ	flow rate

δ, δ_o	film thickness, **Nusselt's laminar film thickness**
η	y/δ
θ	$t - t_w / \Delta t$
κ	thermal diffusivity $(k/C_p \rho)$
λ	latent heat of vaporization
μ	absolute viscosity
ν	kinematic viscosity (μ/ρ)
ξ	x
ρ	density
$\Delta\rho$	$\rho - \hat{\rho}$
τ	$(T - 1) - \dfrac{\lambda}{C_p \Delta t}$

Subscripts

av	average over L
i	interface
s	saturation
t	total (molecular + eddy)
w	wall
1	Deissler's region
2	von Karman's region

Superscripts

*	eddy transport coefficient
^	variable and property in vapor boundary layer.

References

1. Chen, M. M., Trans. ASME, Series C, 83, 48 (1961)

2. Koh, J. C. Y., Sparrow, E. M., and Hartnett, J. P., Int. Jour. Heat Mass Transfer, 2, 69 (1961)

3. Lee, J., ASD-TDR-62-1048, part II, Wright-Patterson AFB (1962)

4. Lee, J., Tech. Memo. ASRCM-63-33, Wright-Patterson AFB (1963) (also submitted to AICHE Journal)

5. Misra, B. and Bonilla, C. F., Chem. Engr. Symp., Series No. 18, 52, 7 (1956)

6. Nusselt, W., Zeit. Ver Deutsch Ingr. 60, 569 (1916)

7. Richtmyer, R. D., Difference Methods for Initial-Value Problems, Interscience Pub. Inc. (1957)

8. Rohsenow, W. M., Weber, J. H., and Ling A. T., Trans ASME, 78, 1637 (1956)

9. Sparrow, E. M. and Gregg, J. L., Trans ASME, Series C, 81, 13 (1959)

10. Colburn, A. P. and Carpenter, E. F., Inst. Mech. Engrs, (ASME), General Discussion on Heat Transfer (1951)

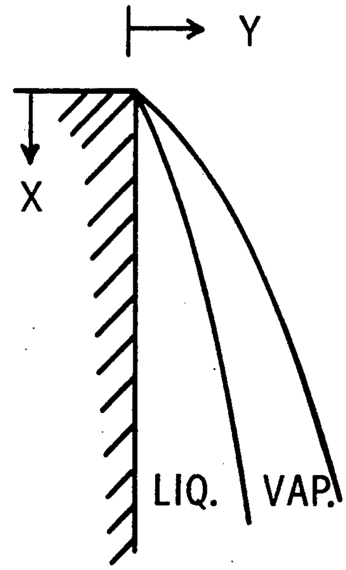

Figure 1 PHYSICAL MODEL & COORDINATES

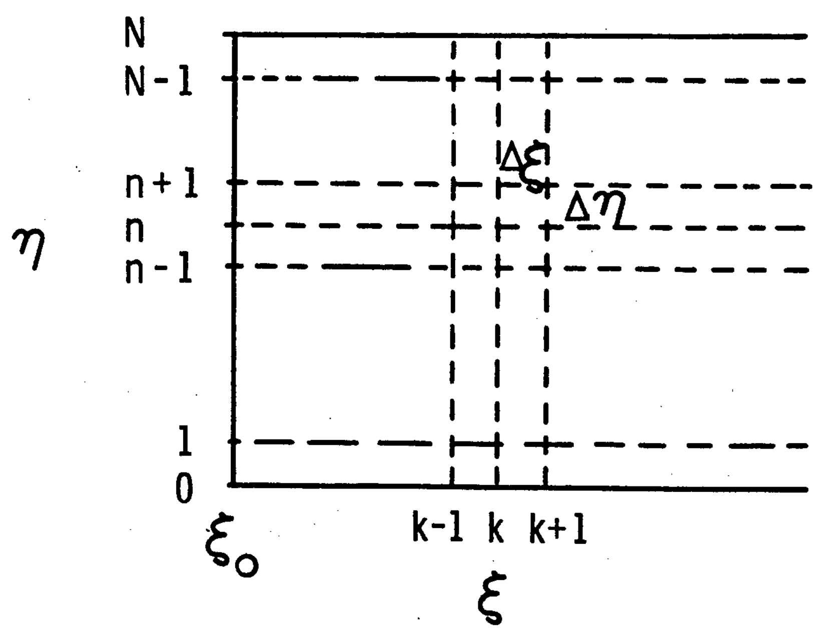

Figure 2 A MESH IN η AND ξ

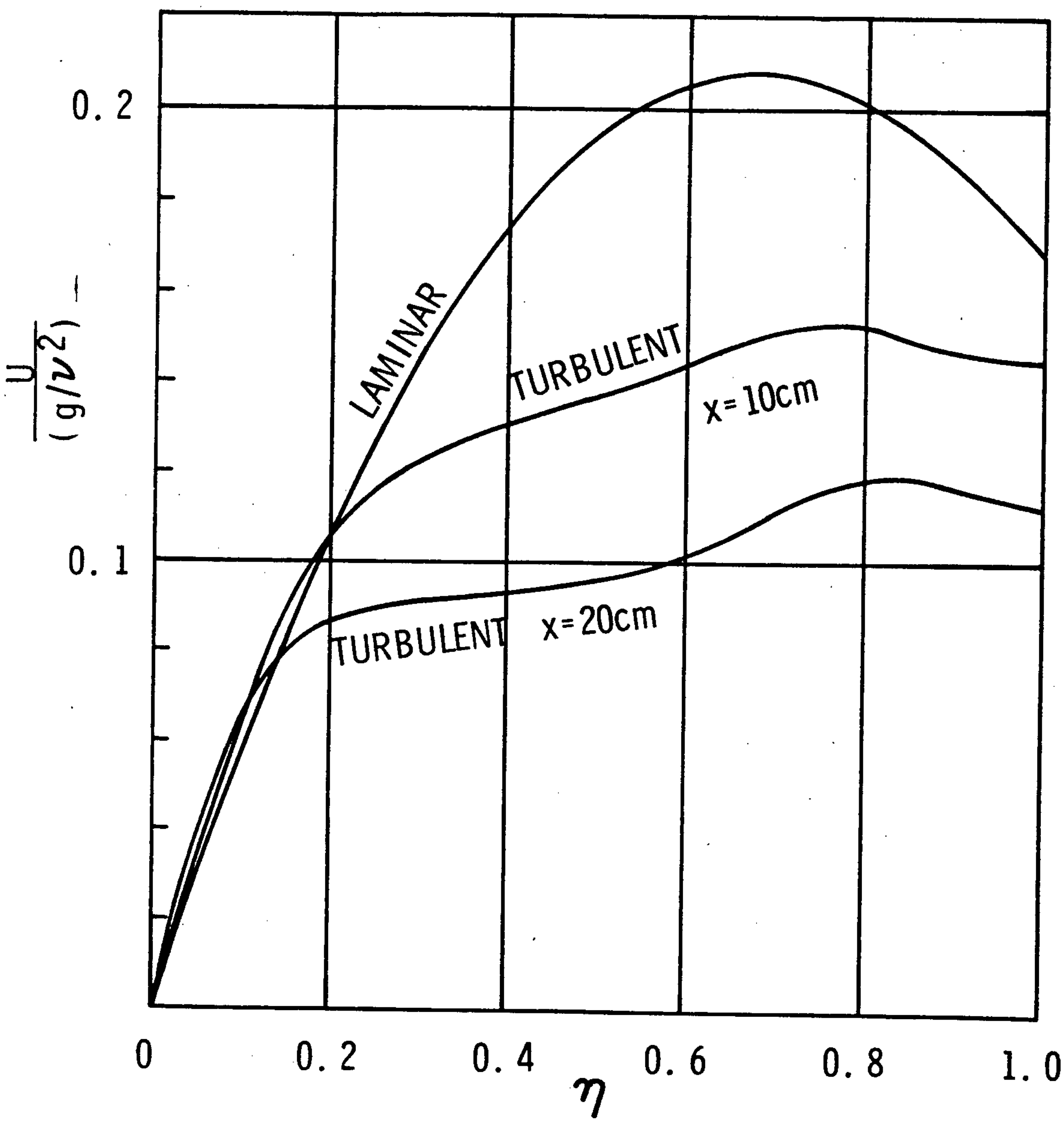

Figure 3 VELOCITY DISTRIBUTION
($P_r = 0.008$ & $C_p \Delta t/\lambda = 0.01$)

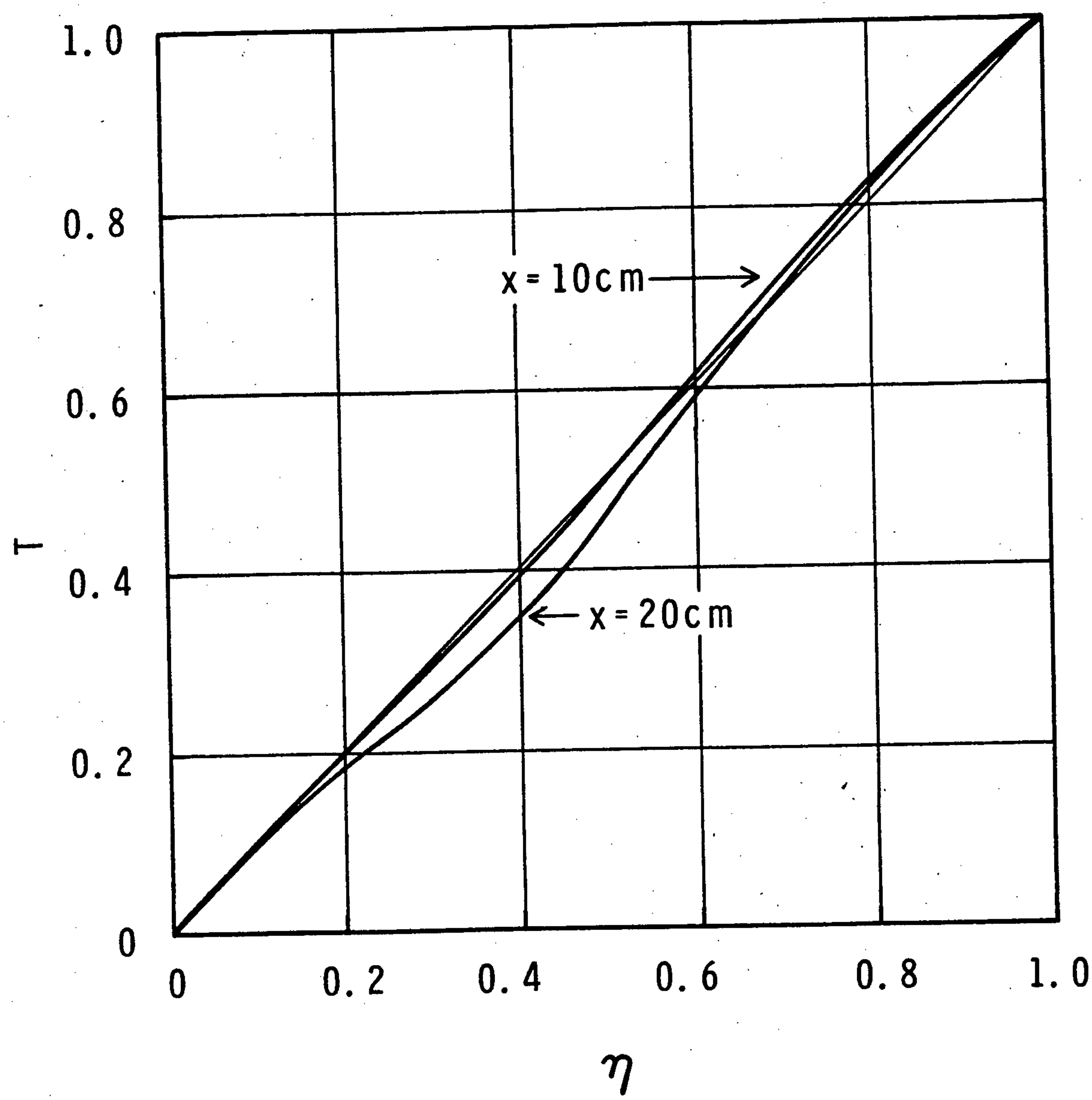

Figure 4 TEMPERATURE DISTRIBUTION
($P_r = 0.008$ & $C_p \Delta t / \lambda = 0.01$)

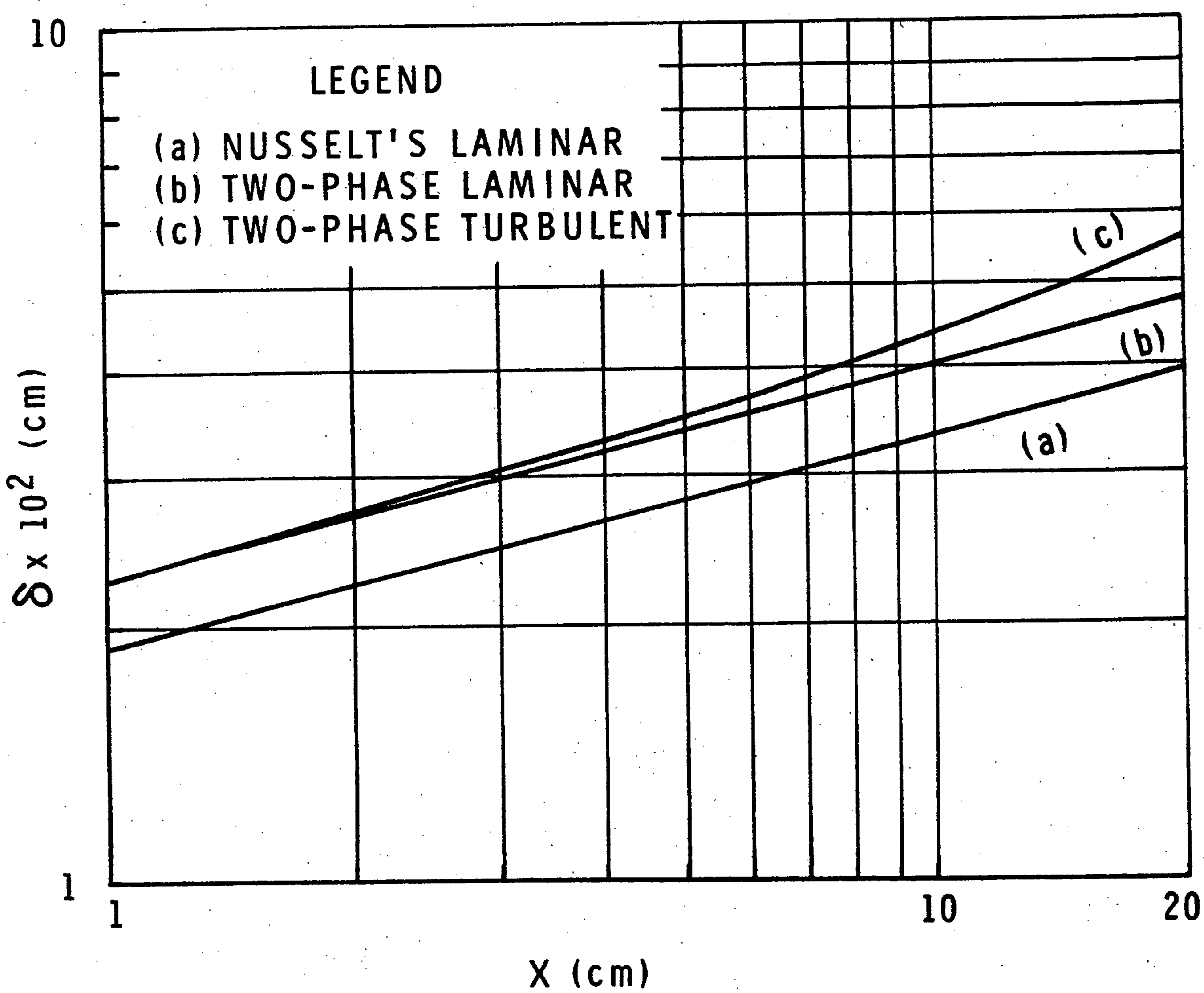

Figure 5 FILM THICKNESS ($P_r = 0.008$ & $C_p\ \Delta t/\lambda = 0.01$)

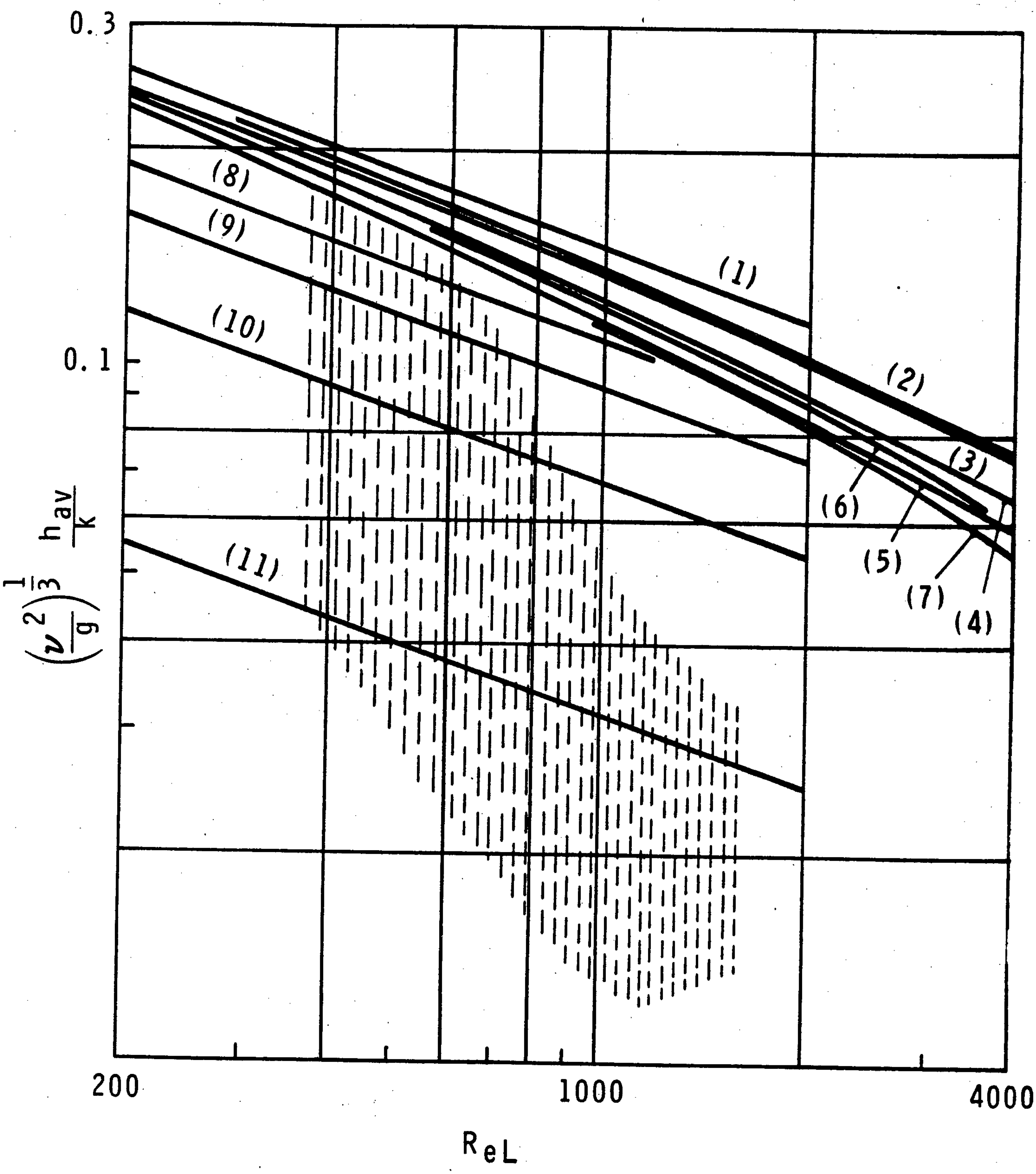

Figure 6 AVERAGE HEAT TRANSFER COEFFICIENT vs REYNOLDS NUMBER

Figure 6 Average Heat Transfer Coefficient vs. Reynolds Number.

Legend

Curve	(1)	Nusselt's laminar (Equation (24))
Curve	(2)	Nusselt's turbulent for P_r=0.01 (Ref.(4))
	(3)	Nusselt's turbulent for P_r=0.001 (Ref.(4))
Curve	(4)	Two-phase laminar for P_r=0.008
	(5)	Two-phase laminar for P_r=0.003
Curve	(6)	Two-phase turbulent for P_r=0.008
	(7)	Two-phase turbulent for P_r=0.003
Curve	(8)	Equation (27) for β =0.4
	(9)	Equation (27) for β =0.5
	(10)	Equation (27) for β =0.6
	(11)	Equation (27) for β =0.66
Shaded Area		Data of Misra and Bonilla (Ref.(5))